

The Fatigue Threshold of Rubber and Its Characterization Using the Cutting Method



Christopher G. Robertson, Radek Stoček, and William V. Mars

Contents

1	Background	58
1.1	General Fatigue Crack Growth Response and the Fatigue Threshold	58
1.2	Molecular Interpretation of Fatigue Threshold/Intrinsic Strength	59
2	Characterization Methods	61
2.1	Near-Threshold Fatigue Crack Growth	62
2.2	Tear Strength of Swollen Materials and/or at High Temperatures	62
2.3	Cutting Method of Lake and Yeoh	64
3	Rubber Formulation Effects	70
3.1	Polymer Type	71
3.2	Crosslinking Effects	72
3.3	Influence of Reinforcing Fillers	74
3.4	Oils/Plasticizers	78
4	Using Fatigue Threshold to Develop Highly Durable Rubber Products	78
5	Conclusions	79
	References	80

Abstract Below a limiting value of tearing energy called the intrinsic strength or fatigue threshold (T_0), cracks will not grow in rubber due to fatigue; hence, this material characteristic is important to understand from both fundamental and practical perspectives. We summarize key aspects of the fatigue threshold, including the Lake-Thomas molecular interpretation of T_0 in terms of fracture of polymer network chains in crosslinked elastomers. The various testing approaches for quantifying T_0 are also discussed, with a focus on the classic Lake-Yeoh cutting method which was

C. G. Robertson (✉) and W. V. Mars
Endurica LLC, Findlay, OH, USA
e-mail: cgrobertson@endurica.com

R. Stoček
PRL Polymer Research Lab, Zlín, Czech Republic

Centre of Polymer Systems, Tomas Bata University in Zlín, Zlín, Czech Republic

recently revived by the introduction of a commercial testing instrument that applies this procedure, the Intrinsic Strength Analyser (ISA). A validation of the cutting method is also given by demonstrating that a 2-h test on the ISA yields a value of T_0 that is essentially identical to the T_0 from near-threshold fatigue crack growth (FCG) measurements that require 7.5 months of continuous testing. Compound formulation effects – polymer type, crosslink density, type and amount of reinforcing fillers, and addition of oils/plasticizers – are examined based on the limited published research in this area and our new results. At the end, some insights are offered into using the fatigue threshold to develop highly durable rubber products.

Keywords Durability · Elastomers · Fatigue crack growth · Intrinsic strength · Materials characterization · Polymer networks

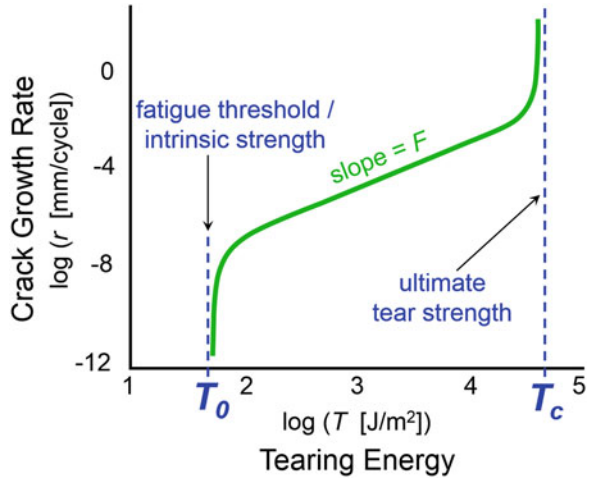
1 Background

It is first essential to define the fatigue threshold which is also referred to as the endurance limit. We will also review the molecular interpretation of this material parameter which will be helpful later when considering the effects of various rubber compounding ingredients. Bhowmick published a nice review article on this topic in 1988 [1], and it is our intent to complement that summary in this section and throughout the chapter while presenting new experimental results and offering some fresh perspectives.

1.1 *General Fatigue Crack Growth Response and the Fatigue Threshold*

Cracks in rubber can grow when a cyclic mechanical deformation is applied, with a crack growth rate, r , that depends on the material, severity of the loading, temperature, and other conditions [2–4]. Although rubber can be formulated to have a wide range of fatigue crack growth (FCG) responses, the general shape of the FCG rate curve is essentially universal. This is shown in Fig. 1 where r is plotted on a log-log plot versus the tearing energy, T , which is also called energy release rate [5]. The FCG curve is a power law response that is bounded on both ends by T_0 and T_c . At the high- T end is the familiar tear strength or critical tearing energy (T_c) of the material. This chapter is focused on the limit at the low- T end of the response which is the fatigue threshold, T_0 . This is an important parameter to quantify for a material. If loads remain below this threshold, then cracks cannot grow, and the material will

Fig. 1 Typical dependence of fatigue crack growth rate on tearing energy (energy release rate) for rubber under fully relaxing conditions (strain cycle oscillates between zero and a peak value at each value of T)



have an infinite fatigue lifetime, in the absence of ozone cracking, thermal-oxidative aging, or other life-limiting changes to the material [6].

In fatigue crack growth testing, the measured crack growth rate r diverges toward zero as T is decreased toward T_0 . The rate is evaluated as $r = dc/dN$, where c is the crack length and N is the number of fatigue cycles. The r range where the FCG curve transitions downward, away from the power law slope, F , is from about 10^{-7} to 10^{-9} mm/cycle. To get a sense for the magnitude of testing time needed at these slow rates, if a typical testing frequency of 10 Hz is considered, it would take about 12 days of continuous testing to observe a tiny 0.1 mm of crack growth when $r = 10^{-8}$ mm/cycle for a material. Also, additional data points would be needed at even slower rates to define the FCG asymptote at T_0 . Due to these generally prohibitive time requirements, it is common to see FCG results reported in the literature that only include the power law region and the upturn near T_c .

1.2 Molecular Interpretation of Fatigue Threshold/Intrinsic Strength

For a crosslinked elastomeric material, the minimum energy for a crack to grow is the energy required to break all the polymer chains that cross the path of the crack. This intrinsic strength is the reason for the divergence of the FCG curve toward $r = 0$ mm/cycle as tearing energy is decreased toward T_0 ; hence, fatigue threshold and intrinsic strength are synonymous. Lake and Thomas [7] derived an expression for intrinsic strength that includes details of the polymer backbone and the extent of crosslinking [1].

$$T_0 = \left[\left(\frac{3}{8} \right)^{1/2} \rho A U \gamma^{1/2} l M_0^{-3/2} \right] M_c^{1/2} = K M_c^{1/2} \quad (1)$$

The polymer backbone characteristics of importance are the chain stiffness (γ), molecular weight of a main chain bond (M_0), the bond length (l), and the bond dissociation energy (U ; bond strength). These are averages across the polymer repeat unit. For example, 1,4-polybutadiene has a repeat unit with four main chain (backbone) bonds and molecular weight of 54 g/mol which leads to $M_0 = 13.5$ g/mol, with l , γ , and U taken as averages of the individual characteristics of the four bonds. Therefore, some of the microstructural details of the polymer backbone are lost in favor of a simpler molecular representation for predicting general trends. The density is represented by ρ , and A is Avogadro's number. For a given type of polymer, all of the molecular characteristics in Eq. 1 are fixed except for M_c and can be combined into a constant K . The molecular weight between crosslinks (M_c) – which is inversely related to crosslink density – is integral to the theory and influences T_0 in two opposite ways. All the bonds in the network chain need to be stretched until they are at the bond dissociation energy before one bond can break, so higher M_c means higher total energy required. The number of bonds in the network chain between two crosslinks is $n = M_c/M_0$, so the energy needed to break the network chain is nU . The other way that M_c plays a role is that longer network chains result in fewer chains that cross the path of the crack. The combination of these two conflicting contributions is a net positive effect leading to T_0 being proportional to $M_c^{1/2}$. Adding more crosslinks in a rubber compound is predicted to decrease the fatigue threshold. The type of polymer is also key, in particular the dependence $T_0 \sim M_0^{-3/2}$. Because the diameter of the chain is proportional to molecular weight per backbone bond, polymer chains with lower M_0 are thinner which means more chains have to be broken per area of crack.

A three-stage schematic is presented in Fig. 2 to illustrate molecular crack growth according to the Lake-Thomas theory: (a) the crack approaches the initially unperturbed network chain coil between crosslinks; (b) with the crosslinks fixed in their location, the advancing crack extends the network chain until it is taut (and all the bonds loaded up to the level of the bond dissociation energy); and (c) one bond in the network chain breaks, allowing the crack to advance and begin to deform the next chain in its path. Though helpful in rationalizing molecular effects on T_0 , this is a highly simplified interpretation. Some limitations of the theory to point out are crosslinks are not allowed to move or break, trapped entanglements are not accounted for, and effects of filler particles are not included. These will be examined further in the later section on rubber formulation effects.

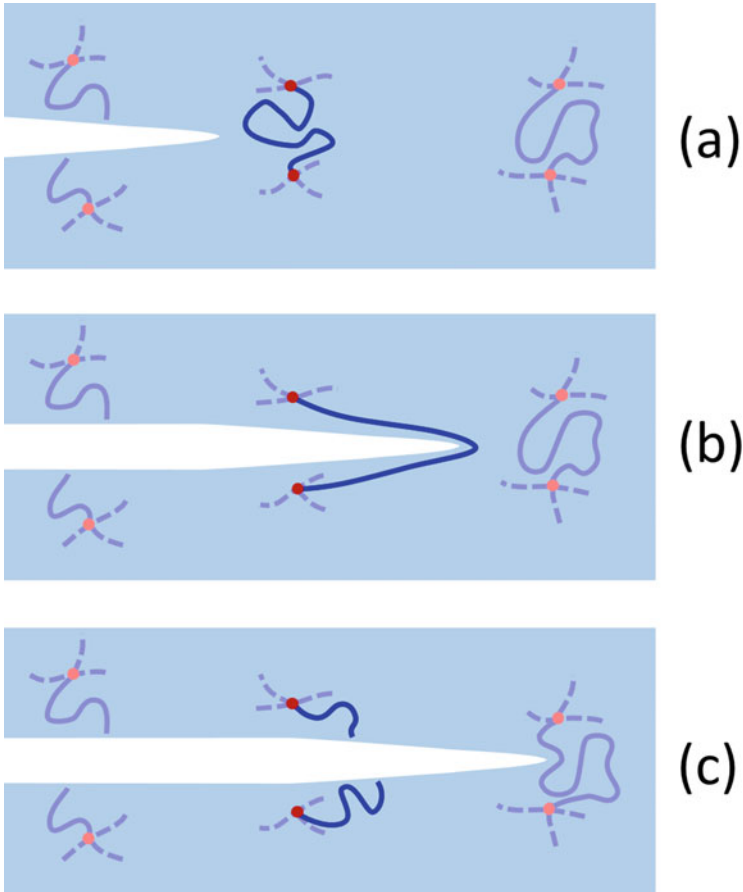


Fig. 2 Illustration of molecular crack growth progression from (a) to (c) for an elastomer network based on the Lake-Thomas model: (a) an initially unperturbed network chain (dark blue line) between two crosslinks (red dots) crosses the path of the advancing crack plane; (b) the advancing crack causes the network chain to become stretched until taut; and (c) the network chain breaks which allows the crack to grow further and begin to deform the next network chain in its path (c)

2 Characterization Methods

The actual energy needed to grow a crack in rubber can be significantly larger than T_0 due to viscoelastic dissipation in a process zone in front of the crack that prevents some of the mechanical energy from getting to the crack tip to break polymer chains. This is the reason that T_c of rubber can be 10 to 10,000 times larger than T_0 and explains the decrease in tear strength as rubber is heated [8]. The concept that tear strength is largely determined by the magnitude of the viscoelastic losses in the crack

tip region is supported by experiments [9, 10]. Rubber would be a weak material without this hysteresis, but it presents a challenge for measuring T_0 .

The energy release rate T of a crack growing at a steady-state rate can be written as the sum of T_0 plus a dissipation-related term T_z [11].

$$T = T_0 + T_z(\dot{\epsilon}, \theta) \quad (2)$$

The strain rate ($\dot{\epsilon}$)- and temperature (θ)-dependent effects are contained entirely in the dissipation term, so that if the process zone dissipation can be eliminated, then the only remaining strength in the material is T_0 . This is the general strategy of the testing methods employed for assessing the fatigue threshold.

2.1 Near-Threshold Fatigue Crack Growth

The direct way to quantify fatigue threshold is to make enough fatigue crack growth measurements near T_0 to define the low- T asymptote in Fig. 1. As T is decreased to values close to T_0 , the size of dissipation zone and hence T_z naturally become small as the rate of crack growth approaches zero. Near-threshold FCG testing is discussed in detail in another chapter in this book by Stoček [12] who rigorously collected data across the entire FCG curve to define T_0 , T_c , and the power law response between these limits for an ethylene-propylene-diene rubber (EPDM) material reinforced with N550 carbon black (CB) at a filler volume fraction (ϕ) of 0.24. The testing conducted in the range $T_0 < T \leq 100 \text{ J/m}^2$ required 7.5 months of continuous instrument time and enabled a determination of $T_0 = 47.7 \text{ J/m}^2$ for this material. This is the original method employed by Lake and Lindley [6] in their work on the fatigue limit. Zhang et al. [13] and Legorju-Jago and Bathias [14] also provide important examples of direct measurement of the fatigue threshold. Very few examples of such measurements are available, presumably due to the lengthy time requirements.

2.2 Tear Strength of Swollen Materials and/or at High Temperatures

It is widely understood that increasing the temperature of rubber causes the tear strength to decrease. The polymer network characteristics, such as bond strength and chain stiffness, are essentially insensitive to temperature, so T_0 does not change significantly as temperature is increased. In contrast, hysteresis decreases as rubber is heated, leading to a smaller T_z and thus a reduced T_c . The difference between T_c and T_0 diminishes with rising temperature which provides an opportunity to approximate T_0 from T_c measured at an elevated temperature. If this estimation approach is used,

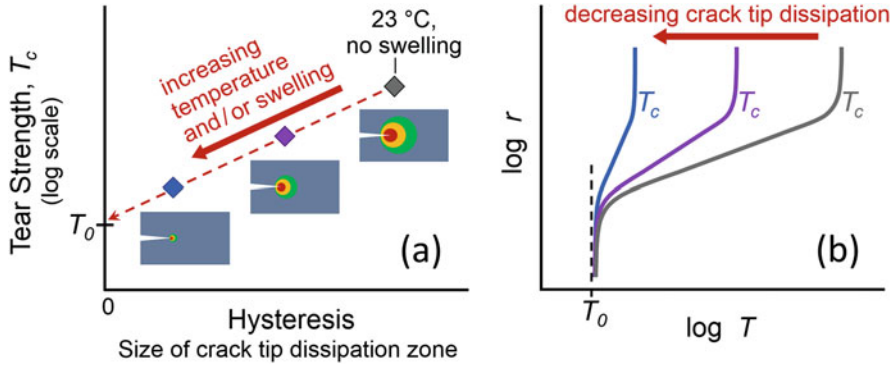


Fig. 3 Schematic of tear strength dependence on crack tip dissipation/hysteresis, as influenced by temperature and swelling (a) and the related crack growth rate curves (b). The dashed red arrow in (a) shows extrapolation to zero hysteresis to approximate T_0

we suggest making tear strength measurements at a few temperatures to generate a plot of T_c versus hysteresis – the latter determined from separate dynamic mechanical analysis testing – and extrapolating to zero hysteresis to evaluate T_0 . This is schematically illustrated in Fig. 3a. It should be emphasized, however, that heating cannot completely eliminate dissipation, and there is a chance that thermal-oxidative aging can take place and change the behavior of the rubber if the temperature is too high. Also, it is not clear whether extrapolation should be performed on a linear or logarithmic T basis.

Another effective way to reduce the size of the crack dissipation process zone in an elastomer is to swell it in a liquid that is a good solvent for the polymer. When swollen, the energy to break a polymer chain is the same, but there are less chains per area of crack compared to the dry rubber. A correction for this chain dilution effect is accordingly required.

$$T_{0,dry} = \lambda^2 T_{0,swollen} \tag{3}$$

The λ is the one-dimensional swelling ratio that describes the change in volume (V) of the material from swelling.

$$\lambda = \left(\frac{V_{swollen}}{V_{dry}} \right)^{1/3} \tag{4}$$

Swelling and elevated temperatures have been used together to approximate T_0 by measuring tear strength at low hysteresis conditions [15–17].

2.3 Cutting Method of Lake and Yeoh

Lake and Yeoh [18] pioneered a cutting method for T_0 characterization that focuses the strain energy density at the crack tip and minimizes dissipation by slowly pushing a sharp blade into the open crack. Based on a crack tip energy balance, they introduced a material parameter called intrinsic cutting energy, $S_{0,c}$, which is equal to T plus an energy release rate for cutting, F .

$$S_{0,c} = T + F \quad (5)$$

Rearranging gives an equation for a line with slope of -1 and intercept $S_{0,c}$ for the dependence of F on T .

$$F = -T + S_{0,c} \quad (6)$$

When applied to the planar tension test specimen, the crack opening energy release rate is $T = Wh$, and the cutting energy release rate is $F = f/t$. W is the strain energy density, h is the gauge height of the specimen, t is the specimen thickness, and f is the cutting force.

Essential to implementing the Lake-Yeoh method is their key finding in Fig. 4 that the T_0 from lengthy near-threshold FCG testing is proportional to the measured $S_{0,c}$.

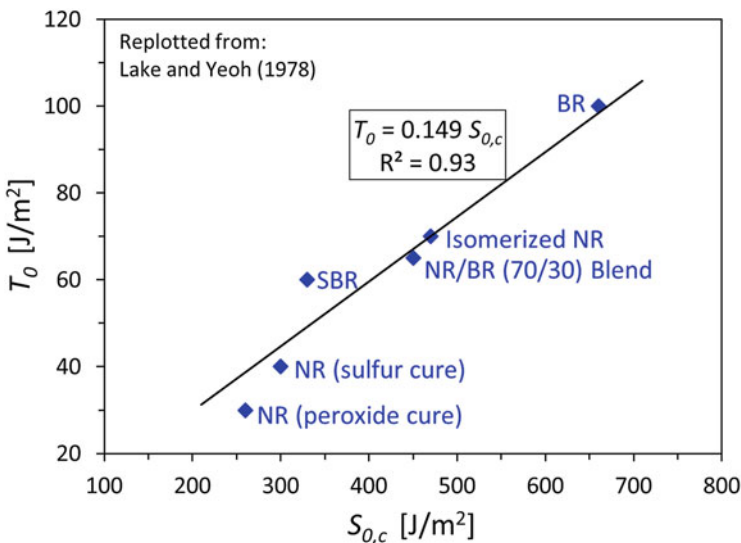


Fig. 4 Lake and Yeoh [18] results for various unfilled elastomers that show correlation between fatigue threshold from very lengthy FCG testing (Y-axis) and the intrinsic cutting energy from the much faster cutting method (X-axis)

$$T_0 = b S_{0,c} \quad (7)$$

Using the cutting method on a control material, for which T_0 is separately known from near-threshold FCG testing, allows the proportionality constant b to be determined. Measuring values of $S_{0,c}$ for both an experimental rubber and the control rubber thus allows T_0 to be quantified for the experimental material. The proportionality b is certainly influenced by the sharpness of the cutting blade. It should also be affected to some extent by the specific friction response between the elastomer material and the metal surface of the blade. This may explain why the linear correlation between T_0 and $S_{0,c}$ is not perfect in Fig. 4, where the unfilled styrene-butadiene rubber (SBR) and natural rubber (NR) materials have T_0 values that are slightly underpredicted and overpredicted, respectively, by the overall linear fit. The material dependence of b needs to be studied further. Application of the Lake-Yeoh cutting method requires a control material, and we use an unfilled SBR compound as a control material in the experiments that are discussed in the next section. For highly accurate measurements of T_0 , for example, to use in developing rubber products with near-infinite fatigue lifetimes, it is recommended to employ a control compound that is similar to the experimental compounds being studied in terms of elastomer type and kind of filler.

2.3.1 Testing Protocol and Data Analysis

Figure 5 shows the experimental set-up of the Lake-Yeoh cutting method applied on the Intrinsic Strength Analyser (ISA) manufactured by Coesfeld GmbH & Co. (Dortmund, Germany). Cutting is performed using an ultra-sharp blade (see

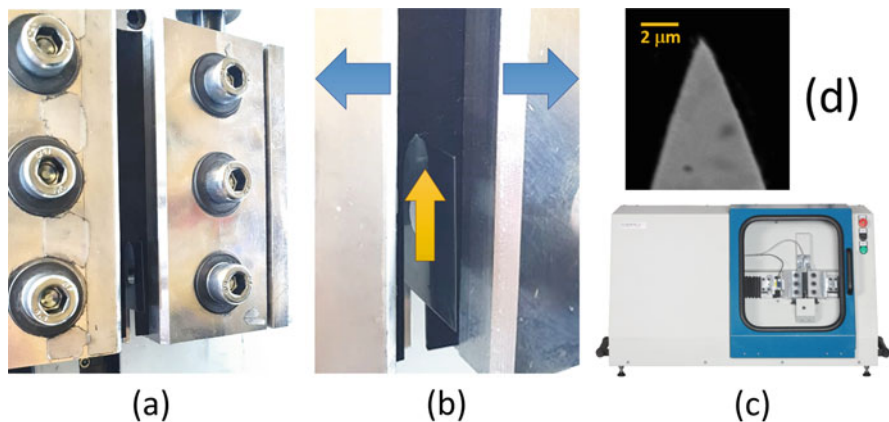


Fig. 5 Pictures of the Coesfeld Intrinsic Strength Analyser (ISA): (a) planar tension specimen in the grips being cut by the blade; (b) close-up view of ultra-sharp blade cutting the rubber specimen with stretching direction (blue arrows) and cutting direction (yellow arrow) indicated; (c) picture of the overall instrument; and (d) scanning electron microscopy image of blade tip

Fig. 6 Plot (a): F versus T cutting method data from the ISA at 23 °C for EPDM filled with CB N550 ($\phi = 0.24$); a line with slope = -1 (solid green line) according to Eq. (6) that contacts the data at the lowest point gives an intercept which is $S_{0,c}$. Plot (b): An alternate presentation of the same data at the lowest cutting speed, where the dependence of the total energy on the planar tension strain used to open the crack is shown, with $S_{0,c}$ defined by the minimum

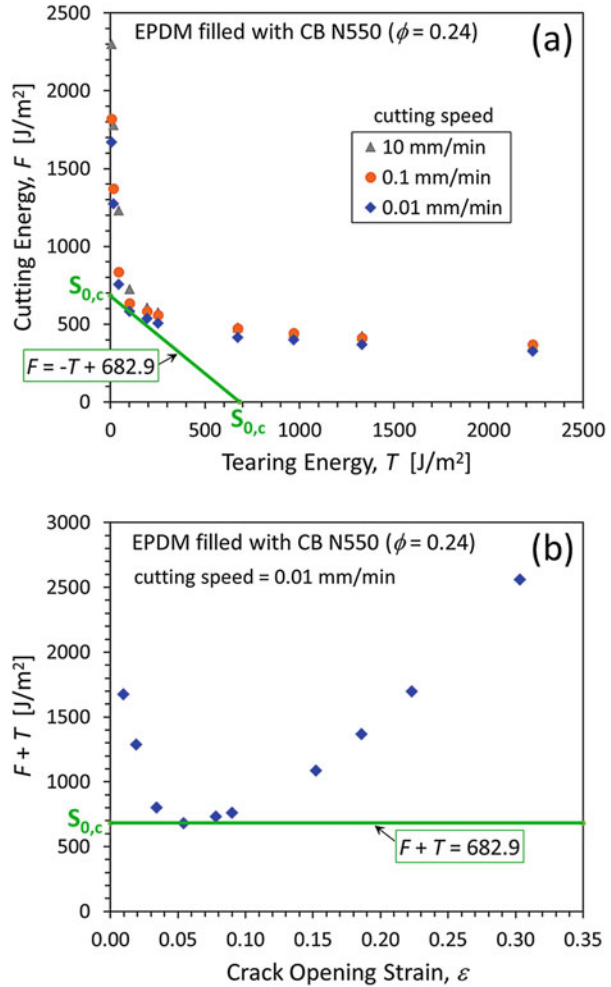


Fig. 5d) that is attached to a sensitive force transducer. Cutting experiments are made for several crack opening strains (T is varied), and more details about the protocol for this series of measurements are given elsewhere [19]. For each T , a fast cutting rate of 10 mm/min is applied for a short time period to develop a well-defined crack path, and then the rate is sequentially slowed down to the rate of 0.01 mm/min to minimize hysteresis near the blade tip. The values of cutting energy release rate, F , used for determining $S_{0,c}$ are from this final slowest cutting rate. This procedure generates a series of F versus T points that are plotted in Fig. 6a for the same CB-filled EPDM ($\phi = 0.24$) studied by Stoček [12]. A line with slope = -1 (Eq. 6) that contacts the data at the lowest point gives the intercept $S_{0,c} = 683$ for this material. Experimental cutting forces are above this line at the lowest T values due to friction of the rubber against the sides of the blade when the crack is not opened much. Contributions from process zone dissipation (T_z becoming significant) explain the points above the line

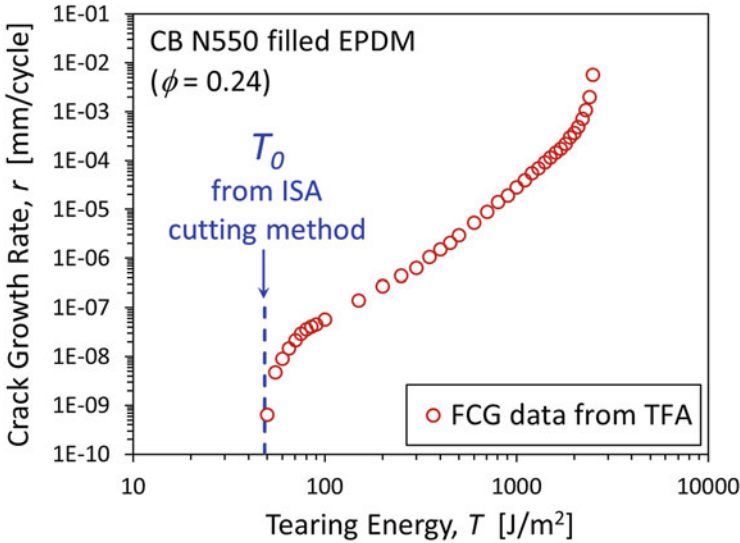


Fig. 7 Comparison of FCG data at 23°C for the CB-filled EPDM from the Tear and Fatigue Analyser (TFA) with separately determined T_0 from the Intrinsic Strength Analyser

Table 1 Fatigue threshold measurements for EPDM filled with CB N550 ($\phi = 0.24$)

Method	T_0 [J/m ²]	Testing time
Near-threshold fatigue crack growth	47.7	7.5 months
ISA cutting method	48.6	2 h ^a

^aISA can also be operated using a targeted testing protocol with total testing time of ~1 h

at the high- T end of the data set. An alternate way to view the results is a plot of the total energy, $F + T$, versus the crack opening strain, with $S_{0,c}$ defined by the minimum (Fig. 6b). An unfilled SBR control material [19] with known $T_0 = 60$ J/m² was also tested, giving a value of 844 J/m² for $S_{0,c}$. This information for the control rubber enabled the determination of $b = 0.0711$ from Eq. (7), then allowing the conversion of $S_{0,c}$ to T_0 for the EPDM compound to yield $T_0 = 48.6$ J/m².

2.3.2 Validation Using Experimental Results and Simulation

The 1978 investigation by Lake and Yeoh [18] showed that the cutting method can be used to assess T_0 , as exemplified in Fig. 4. It is important to verify that our modern application of the cutting method on the Intrinsic Strength Analyser yields a T_0 which is similar to the fatigue threshold defined from fatigue crack growth testing. For this purpose, we consider the EPDM material just discussed with regard to ISA cutting results. EPDM is an appropriate elastomer choice for this comparison, because its largely saturated structure makes it a stable material against oxidation

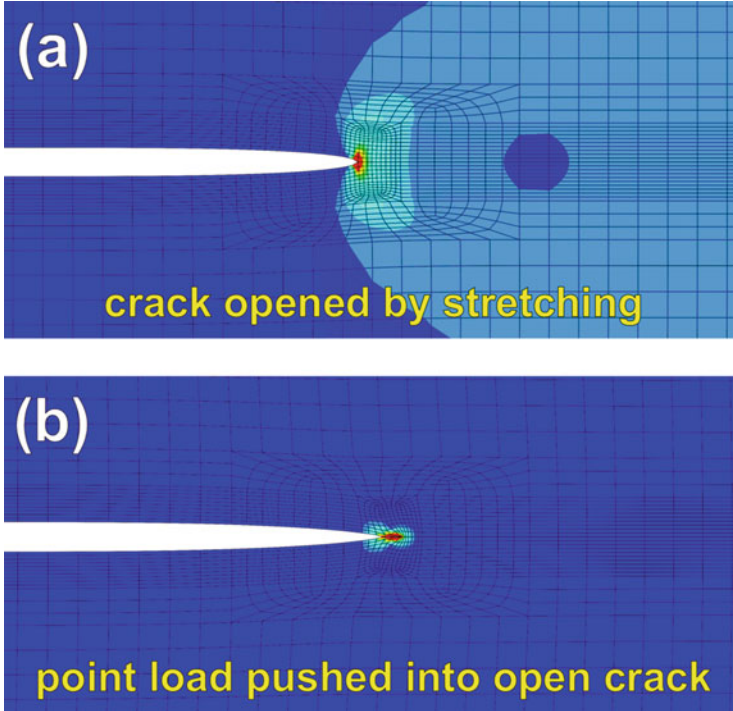


Fig. 8 Abaqus/Standard 2D finite element simulation of strain energy density for a crack in an elastomer that is opened by stretching to a planar tension strain of 0.09 (a) and the subsequent pushing of a point load into the open crack (b). The colors represent a map of different ranges of strain energy density from lower (dark blue) to higher (red) values. Results are from study by Mars et al. [20]

and ozone cracking during the long time period needed for the near-threshold FCG testing. The fatigue crack growth results from Stoček [12] for the EPDM material are presented in Fig. 7, and the data points represent average values from multiple measurements. Also indicated on this figure is the location of the T_0 separately determined using the ISA which is in close proximity to where the crack growth curve turns downward toward infinitesimally small rates. The T_0 from the cutting method test (48.6 J/m^2) is only 1% different than the T_0 from FCG measurements (47.7 J/m^2), as summarized in Table 1. The two characterization approaches produced essentially equivalent T_0 values, but the FCG method involved 7.5 months of testing in contrast to the 2-h ISA test.

A key premise of the Lake-Yeoh cutting approach is that the blade localizes the strain energy density at the crack tip to minimize the dissipation zone in front of the crack. Finite element analysis was recently performed [20] to investigate the validity of this assertion, and selected results from 2D modelling are shown in Fig. 8. When the simulated crack was opened by stretching, a sizeable process zone (i.e., region of magnified stress and strain) in front of the crack was evident. Then a point load was pushed into the open crack to model the effect of the sharp blade in the cutting

method, resulting in substantial reduction in the size of the process zone. This provided strong support for the scientific soundness of the cutting method for evaluating the intrinsic strength of rubber. This modelling research also generated F and T dependencies on crack opening strain and determined that the total process zone energy (sum of F and T) was minimized at a strain of 0.07 (7%). The minimum in Fig. 6b, representing the region of lowest total energy, occurred between the data points collected at strains of 0.054 and 0.078, quite comparable to the simulation minimum.

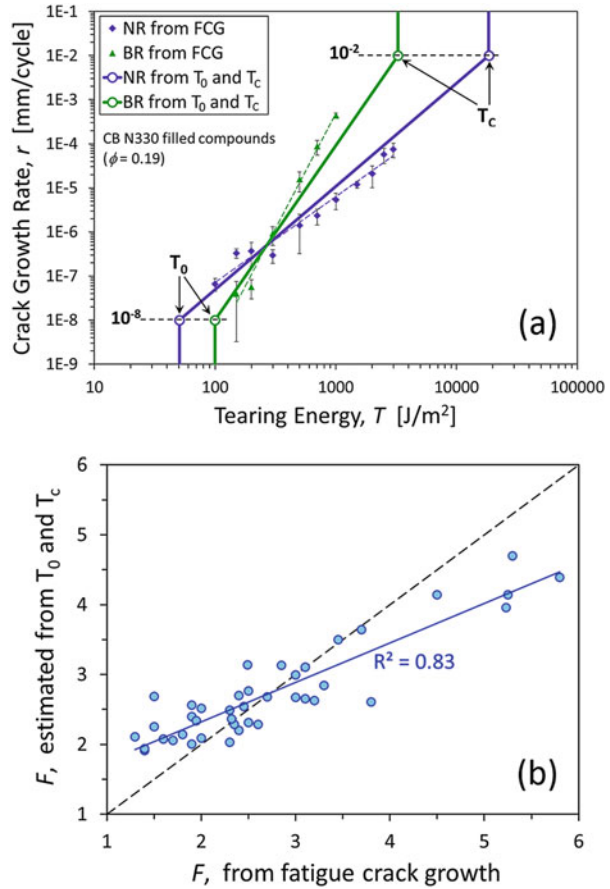
2.3.3 Combining Cutting Method and Tear Testing for Rapid Estimate of Fatigue Crack Growth Curve

After completion of the cutting procedure on the ISA, an optional standard tear test can be performed to determine T_c . The blade is retracted away from the rubber specimen, and then the crack is slowly opened until spontaneous tearing occurs. The ISA therefore can quantify for a rubber specimen the locations of the two ends of the FCG curve that bracket the intermediate power law behavior. Natural rubber (NR) and butadiene rubber (BR) have FCG power law responses that cross over each other. Examples for CB-filled compounds are shown in Fig. 9a [21]. Tear strength is significantly higher for NR (18,490 J/m²) compared to BR (3,270 J/m²), but the material ranking for T_0 is opposite (50.6 J/m² for NR and 99.6 J/m² for BR). We plot T_c and T_0 for both rubbers in Fig. 9a by assuming crack growth rates of $r_c = 10^{-2}$ mm/cycle for T_c and $r_0 = 10^{-8}$ mm/cycle for T_0 . Connecting T_0 and T_c with a line on the log-log plot for each material gives a reasonable approximation for the FCG data between the two limits and reproduces the crossover for NR and BR. This approach can therefore estimate the FCG power law exponent, F , from the ratio of tear strength to intrinsic strength.

$$F \approx \frac{\log(r_c/r_0)}{\log(T_c/T_0)} \approx \frac{6}{\log(T_c/T_0)} \quad (8)$$

A good correlation between this F estimate and the actual F from rigorous FCG measurements is confirmed in Fig. 9b for 41 diverse rubber compounds spanning a large range of F . This quick approach is useful for screening materials and monitoring mixing quality in a rubber factory, but accurate FCG testing is still required for high fidelity fatigue analyses [22].

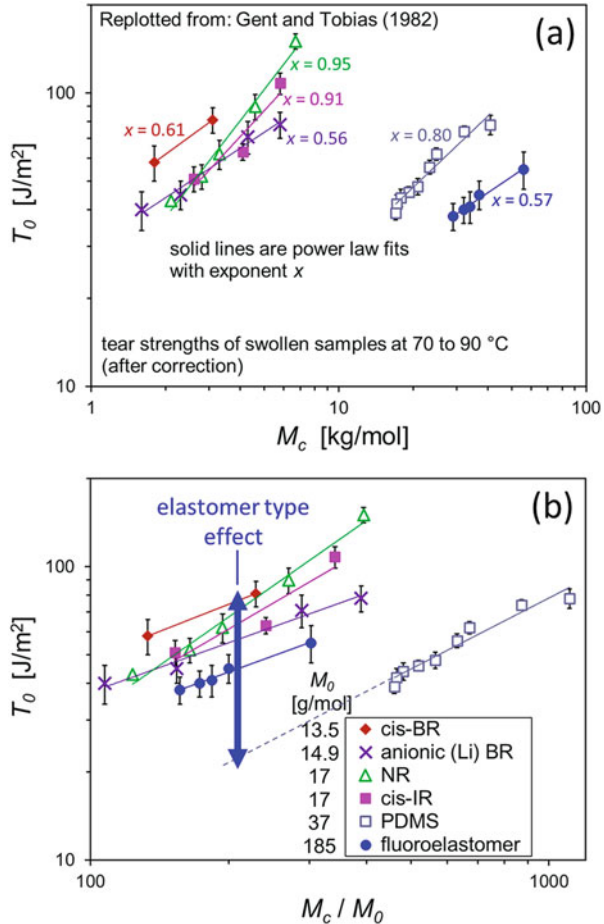
Fig. 9 Plot (a): Fatigue crack growth data from TFA (solid symbols) along with T_0 and T_c data from ISA (open symbols) plotted at r values of 10^{-8} and 10^{-2} , respectively; the thin lines are power law fits to the TFA data, and the thick lines connect the T_0 and T_c points on the log-log plot. Plot (b): Correlation between FCG power law slope determined by two point (T_0 and T_c) ISA method and from actual fitting to FCG data from TFA for data from 41 diverse rubber compounds. Results are replotted from Robertson et al. [21, 22]



3 Rubber Formulation Effects

Rubber formulations are complex mixtures of polymers, reinforcing fillers, curatives, oils/plasticizers, stabilizers, and other additives. The nature and amount of these ingredients, their interactions, and the quality of mixing will affect the compound's durability characteristics, including the fatigue threshold. This complexity gives materials engineers and compound developers the opportunity to create new materials to increase product lifetime. Despite the importance of T_0 , there are only a few published studies that provide data for formulation effects on the fatigue threshold, likely due to the difficulty in measuring T_0 before the commercialization of the cutting method on the ISA. We review these prior investigations and share some of our recent findings in this section.

Fig. 10 Fatigue threshold estimated from swollen tear strength testing at elevated temperatures versus M_c (a) and versus M_c/M_0 (b) for the indicated unfilled elastomers crosslinked with dicumyl peroxide. The elastomer type effect manifests as a vertical shifting in (b) indicated by the blue double-headed arrow. The symbol legend in (b) also applies to (a). Replotted from Gent and Tobias [15]



3.1 Polymer Type

Gent and Tobias [15] used tear testing of swollen samples at temperatures from 70 to 90°C to approximate T_0 for a variety of unfilled polymer types, each studied across a range of M_c by varying the level of peroxide curative. Their results are replotted in Fig. 10a. It is more appropriate to compare crosslinked polymers at constant M_c/M_0 – which is the number of backbone bonds in a network chain between crosslinks (n) – so we compare the fatigue thresholds for the different elastomers as a function of M_c/M_0 in Fig. 10b. The elastomer type effect manifests as a vertical shifting in this plot. The polymer ranking does not exactly follow the Lake-Thomas expectation of $T_0 \sim M_0^{-3/2}$ due to other structural differences between the elastomer types, but the extremes make sense according to this scaling. The heaviest backbones are associated with the fluoroelastomer and poly(dimethylsiloxane) (PDMS) which have the

Table 2 Fatigue threshold values for CB-filled elastomers^{a,b}

Parameter	T_0 [J/m ²]
Natural rubber (NR)	22.2 ± 2.0
Isoprene rubber (IR) ^c	25.7 ± 3.7
Butadiene rubber (BR) ^c	83.5 ± 7.7
Styrene-butadiene rubber (SBR) ^d	63.6 ± 4.7

^aData from our recent ISA cutting method study [23]

^b60 phr CB N339 ($\phi \approx 0.23$) and 1.5 phr sulfur

^cPredominantly cis-1,4 structure

^dEmulsion SBR statistical copolymer with 23.5 wt.% styrene and 14% of butadiene polymerized in 1,2 (vinyl) structure

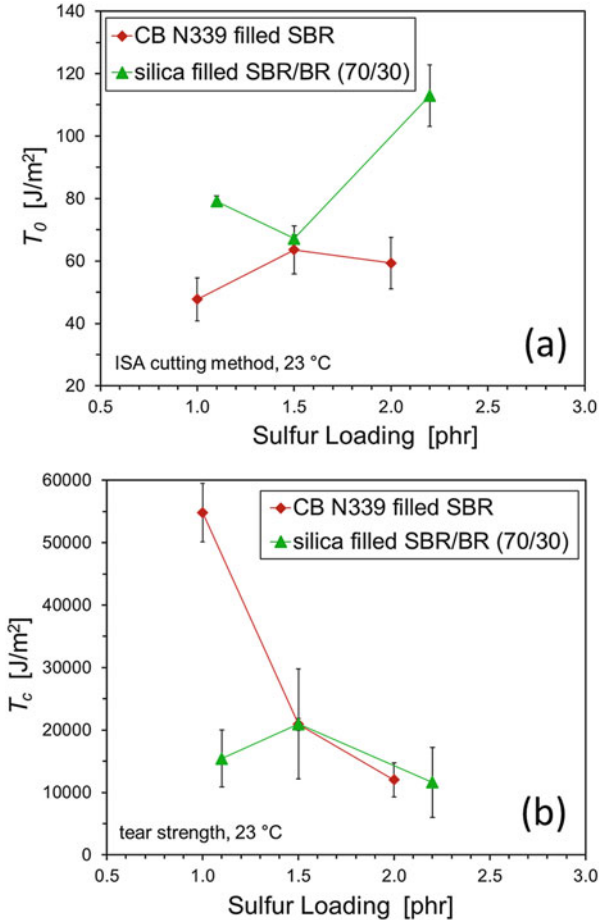
lowest fatigue thresholds at constant M_c/M_0 . At the other extreme is the lightest backbone of cis-1,4-polybutadiene (cis-BR) which has the highest T_0 . Polymer chains with lower M_0 have smaller diameters which translates into more network chains that have to be fractured per area for a crack to grow.

ISA testing of various general-purpose elastomers reinforced with carbon black demonstrated significant influence of polymer type on T_0 (Table 2) [23]. Consistent with the relative fatigue thresholds shown in Fig. 9a, these cutting method results showed that BR exhibited a significantly higher T_0 than was measured for NR. This difference can be qualitatively rationalized based on the Lake-Thomas theory prediction $T_0 \sim M_0^{-3/2}$ (Eq. 1). These two elastomers have similar chain stiffnesses and bond dissociation energies, so the main structural distinction leading to lower T_0 for NR is its higher M_0 (17 g/mol) compared to BR (13.5 g/mol). Also, it was found that the IR and NR materials had similar fatigue thresholds, reflecting their essentially identical cis-1,4-polyisoprene backbones. The T_0 for SBR was intermediate to BR and NR, evidently due to countervailing effects of higher chain stiffness and increased M_0 . The composition of this emulsion SBR (see Table 2) yields $M_0 = 19.6$ g/mol. This is higher than the M_0 for NR and should cause T_0 to be lower for SBR relative to NR in the absence of other structural influences. However, the bulky styrene sidegroup in SBR increases the chain stiffness (γ parameter in Eq. 1) which apparently counters the effect of higher M_0 . The fatigue threshold ranking of BR > SBR > NR in Table 2 agrees with the Lake and Yeoh [18] findings (Fig. 4).

3.2 Crosslinking Effects

The Lake-Thomas interpretation of intrinsic strength is based on the fracture of network chains, which leads to the key model prediction of $T_0 \sim M_c^{1/2}$. According to this anticipation, a higher density of crosslinks produced by adding more curatives in a rubber formulation will reduce M_c and decrease T_0 . This is supported by the results from Gent and Tobias [15] in Fig. 10a which show power law exponents in the range from 0.56 to 0.95 for the different unfilled elastomers examined, reasonably close to the predicted exponent of 0.5. The materials consisted of model formulations with

Fig. 11 Fatigue threshold (a) and tear strength (b) measured using the ISA for the indicated materials as a function of sulfur loading (accelerator-to-sulfur ratio kept constant). The CB N339 loading was $\phi = 0.23$ in the SBR material. For the silica-filled SBR/BR(70/30) compound, the loading of precipitated silica ($165 \text{ m}^2/\text{g}$) was $\phi = 0.19$, and bis [3-(triethoxysilyl)propyl] disulfide (S2 silane; Si266) was added at 8 wt.% relative to the silica amount. Data replotted from our recent studies [23, 24]



only polymer plus dicumyl peroxide, the latter varied from 1 to 5 phr to vary the crosslink density. Their study approximated T_0 using tear strength measurements for swollen specimens at elevated temperatures.

Our recent cutting method evaluations of industrially relevant rubber compounds were less conclusive concerning the influence of crosslinking degree on fatigue threshold [23, 24]. The results are shown in Fig. 11a for two different rubber compositions wherein sulfur concentration was increased to generate different levels of crosslinking while keeping the ratio of accelerator to sulfur constant. There is no clear trend in T_0 versus sulfur level for either material, and the results considered in total are certainly not an endorsement for the Lake-Thomas prediction of a decrease in T_0 from adding more crosslinks. However, the compounds are more complex than the Gent and Tobias model materials and are instead close analogs of materials used in automotive rubber applications. The SBR compound includes CB N339 at a moderately high filler volume fraction, $\phi = 0.23$, and carbon black is known to

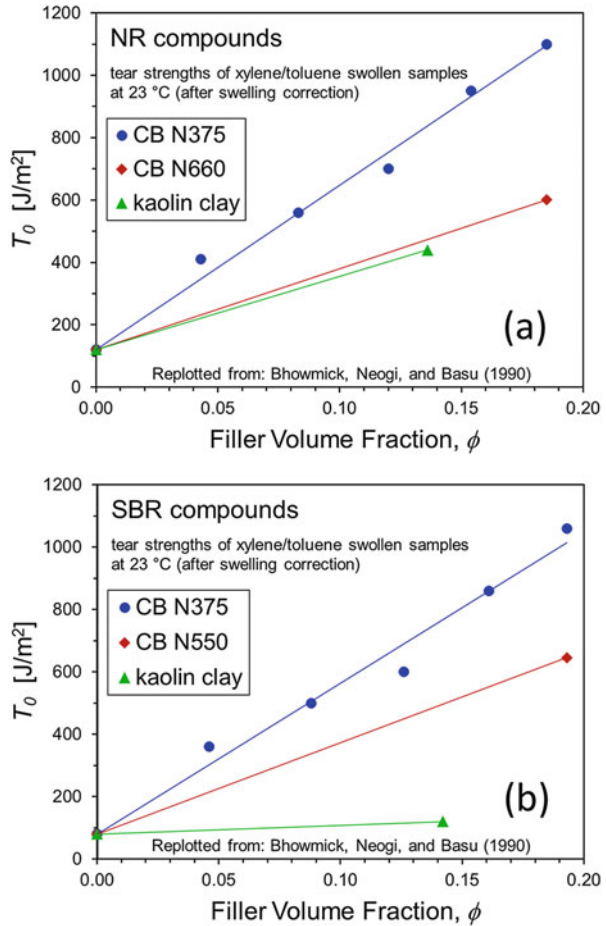
affect vulcanization [25, 26]. The silica-reinforced 70/30 blend of SBR and BR – which is similar to tread compounds used in improved fuel economy passenger car tires – has polymer-silica chemical linkages from bis[3-(triethoxysilyl)propyl] disulfide. This silica-SBR/BR material has a total of 250+ phr in the formulation, of which only 100 phr is the amount of dry elastomers, in clear contrast to 101–105 phr for the simple crosslinked elastomers in Fig. 10.

Crosslink type effects have been observed. Bhowmick, Gent, and Pulford [27] noted that intrinsic strengths of various unfilled elastomers with polysulfidic crosslinks were about two times higher than T_o values for the same elastomers with monosulfidic or -C-C- crosslinks. That study assessed T_o from tear strength of swollen samples at high temperatures. The same effect was found by Gent et al. [28] using the Lake-Yeoh cutting method. This can also be noted in the original Lake and Yeoh results for unfilled NR displayed in Fig. 4 where -C-C- crosslinks from peroxide curing have reduced fatigue threshold compared to polysulfidic crosslinks from sulfur vulcanization. Polysulfidic bonds are significantly weaker than -C-C- and -C-S-C- bonds. This allows polysulfidic crosslinks to break/reform/rearrange during elastomer deformation – which can be considered pseudo-self-healing behavior – to give the well-known advantage of increased tear strength, tensile strength, and fatigue lifetime [29]. Due to limited research, it is not known how the nature of polysulfidic crosslinks can increase the strength at threshold conditions. The Lake-Thomas theory does not allow for crosslink junctions to have lower bond strength than the bonds in the polymer backbone nor the possibility for crosslinks to reform after breaking.

3.3 Influence of Reinforcing Fillers

The majority of commercial applications of rubber employ compounds that contain reinforcing fillers such as carbon black and silica, and filler incorporation is known to increase tear strength and reduce fatigue crack growth rates [2, 10, 30–33]. Only a few studies have considered how filler affects fatigue threshold, however. Bhowmick and coworkers [16] discovered a strong positive influence of CB volume fraction on T_o for NR and SBR compounds (Fig. 12), with a larger effect found for addition of the higher surface area N375 type of CB compared to N550. Kaolin clay gave a lower improvement in NR and nearly no change to T_o in SBR. Up to this point in the chapter, the intrinsic strength data considered from several studies varied across the range from 20 to 150 J/m². The results in Fig. 12 exhibit T_o in excess of 1,000 J/m² at the highest CB N375 concentrations. The authors discussed the general challenge in eliminating hysteresis in filled rubber by use of solvents and/or heating toward quantifying T_o , so it is possible that there were still T_z contributions to the measured tear strengths (Eq. 2). Using the Lake-Yeoh cutting method, Gent et al. [28] showed no effect of adding 50 phr ($\phi = 0.20$) of N330 carbon black to SBR compared to the unfilled material.

Fig. 12 Fatigue threshold estimated from swollen tear strength testing versus filler volume fraction for the indicated filler types in NR (a) and SBR (b). Replotted from Bhowmick, Neogi, and Basu [16]



In Table 3, we summarize new results from the ISA cutting method on the influence of carbon black volume fraction on fatigue threshold of EPDM, where it is evident that increasing CB N550 loading gives a slight decrease in T_0 . These findings are compiled in Fig. 13a along with our recent data on the silica-SBR/BR (70/30) and CB-SBR materials [23, 24] discussed earlier with respect to crosslink density effects. With the exception of the highest silica level, the three filled rubber systems generally show moderately decreasing trends for T_0 as filler amount is increased in the formulation. Tear strength, T_c , increases as expected with filler concentration (Fig. 13b). In view of the opposite filler impacts on T_0 shown in Figs. 12 and 13a, additional research is needed to resolve this important aspect of formulation effects on fatigue threshold.

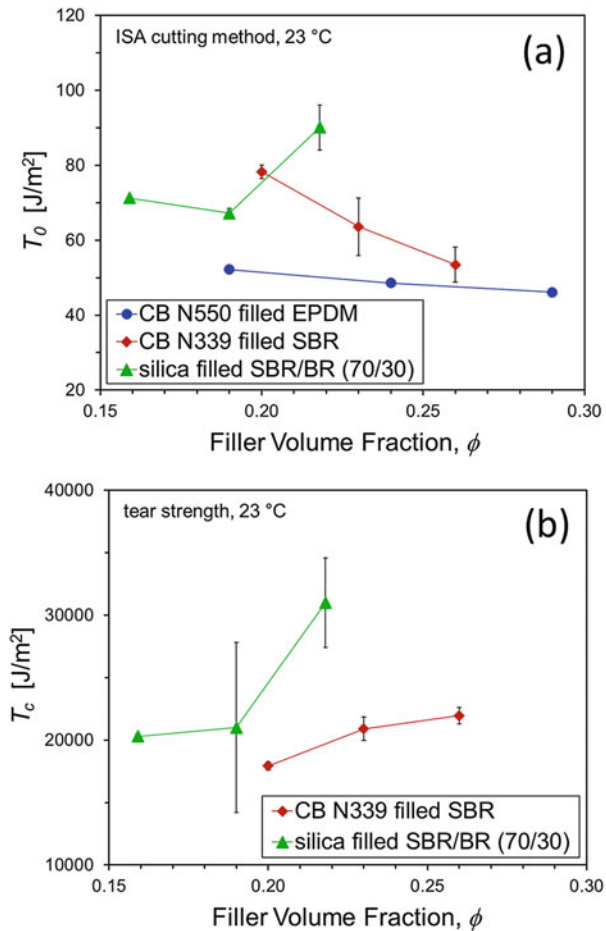
Before attempting to hypothesize about how to extend the molecular insights from the Lake-Thomas theory to address the roles of filler reinforcement and polymer-filler interactions, it is first useful to consider the relative size scales for

Table 3 T_0 results from ISA testing for EPDM filled with CB N550^a

Filler volume fraction, ϕ	T_0 [J/m ²]
0.19	52.2
0.24	48.6
0.29	46.1

^aSame rubber compounds described by Stoczek [12]

Fig. 13 Fatigue threshold (a) and tear strength (b) measured using the ISA for the indicated materials as a function of filler volume fraction. Data from our recent studies [23, 24] and new data for CB-filled EPDM. The crosslinking levels for the CB-SBR and silica-SBR/BR materials are the intermediate concentrations in Fig. 11a. The precipitated silica used in the silica-SBR/BR system had a specific surface area of 165 m²/g, and bis [3-(triethoxysilyl)propyl] disulfide (S2 silane; Si266) was added at 8 wt.% relative to the silica amount



network chains and filler particles. Typical crosslink densities in elastomers are associated with distances between crosslinks that are less than 10 nm in the unstretched state [34, 35]. Measured chain dimensions in theta conditions for 1,4-polyisoprene (NR, IR) and 1,4-polybutadiene (BR) are characterized by essentially the same expression for the dependence of hydrodynamic radius on molecular

weight [36]: $R_H \approx 0.03 M^{1/2}$, with M expressed in g/mol and R_H in units of nm. This can be used to estimate the size of the chain coil between crosslinks by substituting M_c for M . This gives coil diameters from 3 to 6 nm for M_c values in the common range from 2,000 to 10,000 g/mol (see data ranges in Fig. 10a). Comparable end-to-end distances of 3–7 nm can be determined using chain statistics for BR across the same span of M_c [34]. The standard N110, N339, and N550 grades of carbon black have average primary particle diameters of 17, 26, and 53 nm, respectively, and aggregate diameters of 54, 75, and 139 nm [37]. Therefore, even the smallest nanostructured carbon blacks that are used to reinforce rubber (e.g., N110) are characterized by primary particles that are more than twice the size of the network chain coil, and the aggregates of fused primary particles have diameters that are about ten times the distance between crosslinks. The size mismatch is depicted in Fig. 14. This greatly complicates the crack growth process beyond the simple Lake-Thomas molecular interpretation illustrated previously (Fig. 2). Certainly, physical adsorption or chemical bonding of a portion of the polymer chain to the surface of a particle will affect the mechanics of near-threshold crack growth. Perhaps more important to address is how the crack – which is able to progress forward between crosslink points that are a few nanometers apart according to the Lake-Thomas view – navigates around or through a much larger rigid filler aggregate. Another complexity is that swelling of a particle-reinforced elastomer network is not a simple chain dilution effect [38–40], and temperature affects filler networking and polymer-filler

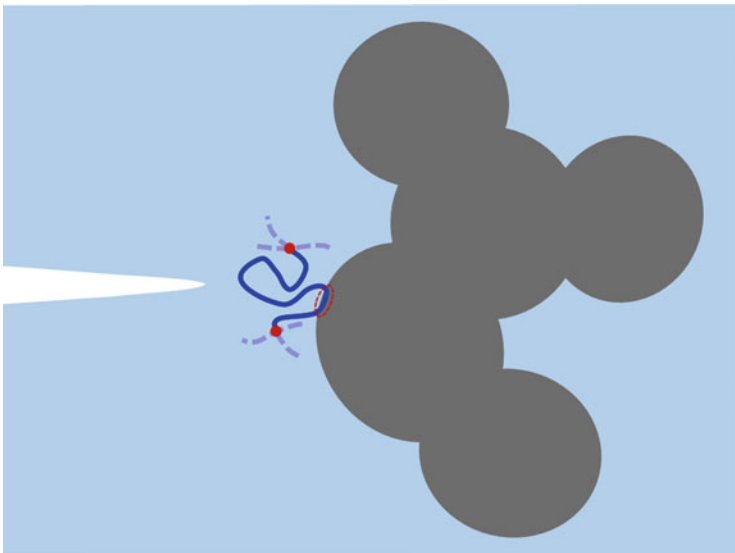


Fig. 14 Depiction of polymer network chain (dark blue line) between two crosslinks (red dots) that is in front of an advancing crack. The chain is adsorbed or bonded onto the surface of a filler aggregate (gray) which is composed of five primary particles fused together, with the region of polymer-filler interaction circled (red dashed line). See discussion text for relative sizes of polymer network chain and filler aggregate

interactions [41–44], so quantifying T_0 from tear strength testing of swollen samples at elevated temperatures may not be appropriate for filled rubber.

3.4 Oils/Plasticizers

To our knowledge, there have not been any systematic studies of the impacts of process oils, plasticizers, or other low molecular weight liquid additives on the fatigue threshold of rubber. We can get some insights by treating oil in a formulation in the same manner as the swelling correction in Eqs. 3 and 4, since oil has a comparable effect of diluting the polymer network chains. The one-dimensional swelling ratio for adding an oil to a dry polymer can be expressed as:

$$\lambda = \left(1 + \frac{w_o/\rho_o}{w_p/\rho_p} \right)^{1/3} \quad (9)$$

The w_o and w_p represent the weights in phr of the oil and dry polymer within the formulation, and ρ_o and ρ_p are their respective densities. Elastomers such as SBR and EPDM are often blended with oil by synthetic rubber manufacturers. A common oil concentration for oil extended elastomers is 37.5 phr per 100 phr of dry polymer. This amount of oil dilution causes a 19% reduction in T_0 according to Eqs. (3) and (9) if the oil and polymer have the same density. To increase fatigue threshold, the levels of process oils and other non-reactive low molecular weight liquids in a compound should be decreased, provided that reducing/eliminating these ingredients can be accomplished while still maintaining proper filler dispersion and acceptable rubber processability.

4 Using Fatigue Threshold to Develop Highly Durable Rubber Products

The main industrial interest in quantifying crack growth properties of elastomers is to use those insights to develop durable products. For product application conditions where $T > T_0$ and fatigue cracking will occur in a rubber component, modern fatigue analysis software for finite element analysis can be used to predict lifetime by incorporating concepts of critical plane analysis and integrated fatigue crack growth rate function [45–47]. The development approach is to create a material and design geometry combination that will give predicted cycles to failure in excess of the desired product lifetime for the complex application loading cycle and other use conditions. In this context, knowledge of the fatigue threshold is also useful for identifying non-damaging events in lengthy road load signals experienced by automotive rubber components. Sub-threshold events can be removed from consideration during testing and simulation efforts [45, 48].

An alternative, very conservative strategy is to produce a combination of design and material behavior that interplay with the loading situation to operate at sub- T_0 conditions where fatigue crack growth cannot take place. Accurate values of T_0 for the material and the effective tearing energy (T) associated with the rubber component operation must both be known in order to ensure $T < T_0$. The tearing energy can be expressed as [47, 49–52]:

$$T = 2 k W c \quad (10)$$

Detailed discussions about the precise value of k are found in the chapters of Wunde et al. and Windslow et al. in this book [51, 52]. For simplicity, we use the approximate value $k = \pi$ [47]. The strain energy density (W) is the area under the stress versus strain response for the material experiencing the applied duty cycle in the product, so it is a combination of hyperelastic stress-strain behavior of the material, the part geometry, and deformation conditions. Finite element analysis is invaluable for assessing W throughout a rubber product design experiencing the loading conditions. At the start of fatigue, the crack size, c , of importance is the crack precursor size, c_0 . The goal is then to find a material and design combination that satisfies:

$$2 \pi W c_0 < T_0 \quad (11)$$

Crack precursors are sometimes called intrinsic flaws or defects, and they can come from undispersed filler agglomerates, hard contaminants in raw materials, and other aspects of the compound and its morphology/microstructure [53–55]. Crack precursor size is not a single number but rather a distribution [55] which should be considered with respect to failure statistics when selecting which c_0 to use in the product engineering criterion represented by Eq. (11). The possibility that fatigue threshold deteriorates with aging needs to be explored by testing T_0 of the material candidate after aging at relevant conditions. Also, any aging-induced changes to the rubber stiffness will affect W and should be included in the analysis toward keeping $T < T_0$ throughout the intended product lifetime.

5 Conclusions

We summarized key aspects of the fatigue threshold of rubber. Knowledge of this important material parameter can be used to develop rubber products with infinite fatigue lifetime, not considering other possible life-limiting changes to the material from aging, ozone cracking, and the like. The various testing approaches were discussed, with a focus on the well-established Lake-Yeoh cutting method that is implemented on the ISA. The cutting method was validated by demonstrating that a 2-h test on the ISA yields a T_0 that is nearly identical to the T_0 value from near-threshold fatigue crack growth measurements that require 7.5 months of continuous

testing. Finite element analysis of the cutting method provided support for the key premise that the blade localizes the strain energy density near the crack tip, and the simulations predicted a minimum in the total energy (tearing plus cutting) at a crack opening strain of 0.07 which matched the minimum in the experimental results.

The limited number of published studies on rubber formulation effects was reviewed, and the results were compared with our new data. The elastomer type has a clear impact on T_0 , and lighter, smaller-diameter polymer chains have an advantage. Conflicting results exist for the dependencies of fatigue threshold on crosslink density and filler reinforcement, possibly due to differences in results from the cutting method versus tear testing of swollen specimens at high temperatures. For the latter characterization approach, it is particularly challenging to reach vanishing hysteresis conditions for rubber compounds that contain reinforcing fillers. More research is needed to clarify the various influences of rubber compound ingredients on T_0 .

The Lake-Thomas model interprets T_0 in terms of fracture of elastomer network chains and is useful in rationalizing impacts of polymer structure, addition of oils/plasticizers to a compound, and crosslink density. Extending the Lake-Thomas conceptual framework to particle-reinforced rubber will require more than just adding polymer-filler interactions and related mobility effects into the physics. The size scales of common carbon black and precipitated silica particles are significantly larger than the size of a polymer network chain between crosslinks, which requires cracks to either go around the nano-structured filler aggregates or fracture them.

There are many interesting and innovative materials technologies such as sacrificial bonds [56], designer microstructures [57], self-healing functionalities [58], and double networks [59] that can increase intrinsic strength and retard crack growth in elastomeric materials. The translation of these basic research concepts and other materials science ideas into commercial rubber products with enhanced durability will require fast, reliable characterization of the fatigue threshold, and the Lake-Yeoh cutting method on the Intrinsic Strength Analyser will undoubtedly play an important role.

Acknowledgments This research was supported in part by the Ministry of Education, Youth and Sports of the Czech Republic – DKRVO (RP/CPS/2020/004). We thank Joshua R. Goossens from DrIV Inc. (Milan, OH) and Dr. Nihat Isitman from Goodyear Tire & Rubber Company (Akron, OH) for collaborating in the ISA investigations of compounding effects that are described in previous works [23, 24] and replotted in this chapter.

References

1. Bhowmick AK (1988) Threshold fracture of elastomers. *J Macromol Sci Part C Polym Rev* 28:339–370
2. Mars WV, Fatemi A (2004) Factors that affect the fatigue life of rubber: a literature survey. *Rubber Chem Technol* 77:391–412
3. Harbour RJ, Fatemi A, Mars WV (2007) The effect of a dwell period on fatigue crack growth rates in filled SBR and NR. *Rubber Chem Technol* 80:838–853

4. Stadlbauer F, Koch T, Archodoulaki V-M, Planitzer F, Fidi W, Holzner A (2013) Influence of experimental parameters on fatigue crack growth and heat build-up in rubber. *Materials* 6:5502–5516
5. Stoček R, Horst T, Reincke K (2016) Tearing energy as fracture mechanical quantity for elastomers. *Adv Polym Sci* 275:361–398
6. Lake GJ, Lindley PB (1965) The mechanical fatigue limit for rubber. *J Appl Polym Sci* 9:1233–1251
7. Lake GJ, Thomas AG (1967) The strength of highly elastic materials. *Proc R Soc Lond A* 300:108–119
8. Sakulkaew K, Thomas AG, Busfield JJC (2013) The effect of temperature on the tearing of rubber. *Polym Test* 32:86–93
9. Tsunoda K, Busfield JJC, Davies CKL, Thomas AG (2000) Effect of materials variables on the tear behaviour of a non-crystallising elastomer. *J Mater Sci* 35:5187–5198
10. Bhattacharyya S, Lodha V, Dasgupta S, Mukhopadhyay R, Guha A, Sarkar P, Saha T, Bhowmick AK (2019) Influence of highly dispersible silica filler on the physical properties, tearing energy, and abrasion resistance of tire tread compound. *J Appl Polym Sci* 136:47560
11. Andrews EH (1963) Rupture propagation in hysterical materials: stress at a notch. *J Mech Phys Solids* 11:231–242
12. Stoček R (2021) Some revision of fatigue crack growth characteristics of rubber. In: Heinrich G, Stoček R, Kipscholl R (eds) *Fatigue crack growth in rubber materials: experiments and modelling*. Springer, Berlin
13. Zhang E, Bai R, Morelle XP, Suo Z (2018) Fatigue fracture of nearly elastic hydrogels. *Soft Matter* 14:3563–3571
14. Legorju-Jago K, Bathias C (2002) Fatigue initiation and propagation in natural and synthetic rubbers. *Int J Fatigue* 24:85–92
15. Gent AN, Tobias RH (1982) Threshold tear strength of elastomers. *J Polym Sci Polym Phys Ed* 20:2051–2058
16. Bhowmick AK, Neogi C, Basu SP (1990) Threshold tear strength of carbon black filled rubber Vulcanizates. *J Appl Polym Sci* 41:917–928
17. Mazich KA, Samus MA, Smith CA, Rossi G (1991) Threshold fracture of lightly crosslinked networks. *Macromolecules* 24:2766–2769
18. Lake GJ, Yeoh OH (1978) Measurement of rubber cutting resistance in the absence of friction. *Int J Fract* 14:509–526
19. Robertson CG, Stoček R, Kipscholl C, Mars WV (2019) Characterizing the intrinsic strength (fatigue threshold) of natural rubber/butadiene rubber blends. *Tire Sci Technol* 47:292–307
20. Mars WV, Robertson CG, Stoček R, Kipscholl C (2019) Why cutting strength is an indicator of fatigue threshold. In: Huneau B, Le Cam J-B, Marco Y, Verron E (eds) *Constitutive models for rubber XI*. CRC Press, Taylor & Francis Group, London, pp 351–356
21. Robertson CG, Suter JD, Bauman MA, Stoček R, Mars WV (2020) Finite element modeling and critical plane analysis of a cut-and-chip experiment for rubber. *Tire Sci Technol*. <https://doi.org/10.2346/tire.20.190221>
22. Robertson CG, Stoček R, Kipscholl R, Mars WV (2019) Characterizing durability of rubber for tires. *Tire Technol Int Ann Rev*:78–82
23. Robertson, C.G., Goossens, J.R., Mars, W.V. (2019) Using the laboratory cutting method for predicting long-term durability of elastomers. In: Paper D15, presented at the fall 196th technical meeting of the rubber division, ACS, Cleveland, OH, Oct 10–12, 2019
24. Isitman N, Stoček R, Robertson CG (2020) Influences of compounding attributes on intrinsic strength and tearing behavior of model tread rubber compounds. In: Paper scheduled to be presented at the 197th technical meeting of the rubber division, ACS, Independence, OH, April 28–30, 2020 (Presentation slides made available online due to meeting cancellation for COVID-19 precaution)

25. Hosseini SM, Razzaghi-Kashani M (2018) Catalytic and networking effects of carbon black on the kinetics and conversion of sulfur vulcanization in styrene butadiene rubber. *Soft Matter* 14:9194–9208
26. Blokh GA, Melamed CL (1961) The interaction of carbon black with sulfur, MBT and TMTD in vulcanization. *Rubber Chem Technol* 34:588–599
27. Bhowmick AK, Gent AN, Pulford CTR (1983) Tear strength of elastomers under threshold conditions. *Rubber Chem Technol* 56:226–232
28. Gent AN, Lai S-M, Nah C, Wang C (1994) Viscoelastic effects in cutting and tearing of rubber. *Rubber Chem Technol* 67:610–618
29. Rader CP (2001) Chapter 7. Vulcanization of rubber – A. sulfur and non-peroxides. In: Baranwal KC, Stephens HL (eds) *Basic elastomer technology*. The rubber division. ACS, Akron, pp 165–190
30. Klüppel M (2009) The role of filler networking in fatigue crack propagation of elastomers under high-severity conditions. *Macromol Mater Eng* 294(2):130–140
31. Vaikuntam SR, Bhagavatheswaran ES, Xiang F, Wiefner S, Heinrich G, Das A, Stöckelhuber KW (2020) Friction, abrasion and crack growth behavior of in-situ and ex-situ silica filled rubber composites. *Materials* 13:270
32. Sridharan H, Guha A, Bhattacharyya S, Bhowmick AK, Mukhopadhyay R (2019) Effect of silica loading and coupling agent on wear and fatigue properties of a tread compound. *Rubber Chem Technol* 92:326–349
33. Rooj S, Das A, Morozov IA, Stöckelhuber KW, Stoček R, Heinrich G (2013) Influence of “expanded clay” on the microstructure and fatigue crack growth behavior of carbon black filled NR composites. *Compos Sci Technol* 76:61–68
34. Heinrich G, Vilgis TA (1993) Contribution of entanglements to the mechanical properties of carbon black-filled polymer networks. *Macromolecules* 26:1109–1119
35. Robertson CG, Wang X (2004) Nanoscale cooperative length of local segmental motion in polybutadiene. *Macromolecules* 37:4266–4270
36. Fetters LJ, Hadjichristidis N, Lindner JS, Mays JW (1994) Molecular weight dependence of hydrodynamic and thermodynamic properties for well-defined linear polymers in solution. *J Phys Chem Ref Data* 23:619–640
37. Hess WM, McDonald GC (1983) Improved particle size measurements on pigments for rubber. *Rubber Chem Technol* 56:892–917
38. Kraus G (1963) Swelling of filler-reinforced vulcanizates. *J Appl Polym Sci* 7:861–871
39. Busfield JJC, Thomas AG, Yamaguchi K (2004) Electrical and mechanical behavior of filled elastomers 2: the effect of swelling and temperature. *J Polym Sci B Polym Phys* 42:2161–2167
40. Elhaouzi F, Mdarhri A, Brosseau C, El Aboudi I, Almaggoussi A (2019) Effects of swelling on the effective mechanical and electrical properties of a carbon black-filled polymer. *Polym Bull* 76:2765–2776
41. Arai K, Ferry JD (1986) Temperature-dependence of viscoelastic properties of carbon-black-filled rubbers in small shearing deformations. *Rubber Chem Technol* 59:592–604
42. Mujtaba A, Keller M, Ilich S, Radosch HJ, Beiner M, Thurn-Albrecht T, Saalwächter K (2014) Detection of surface-immobilized components and their role in viscoelastic reinforcement of rubber–silica Nanocomposites. *ACS Macro Lett* 3:481–485
43. Sternstein SS, Amanuel S, Shofner ML (2010) Reinforcement mechanisms in Nanofilled polymer melts and elastomers. *Rubber Chem Technol* 83:181–198
44. Warasitthinon N, Genix A-C, Sztucki M, Oberdisse J, Robertson CG (2019) The Payne effect: primarily polymer-related or filler-related phenomenon? *Rubber Chem Technol* 92:599–611
45. Barbash KP, Mars WV (2016) Critical plane analysis of rubber bushing durability under road loads. SAE technical paper, no. 2016-01-0393
46. Mars WV, Wei Y, Hao W, Bauman MA (2019) Computing Tire component durability via critical plane analysis. *Tire Sci Technol* 47:31–54
47. Mars WV (2021) Critical plane analysis of soft materials. In: Heinrich G, Stoček R, Kipscholl R (eds) *Fatigue crack growth in rubber materials: experiments and modelling*. Springer, Berlin

48. Mars WV, Suter JD (2019) Breaking the computational barrier to simulating full road load signals in fatigue. In: Paper C08, presented at the fall 196th technical meeting of the rubber division, ACS, Cleveland, OH, Oct. 10–12, 2019
49. Aït-Bachir M, Mars WV, Verron E (2012) Energy release rate of small cracks in hyperelastic materials. *Int J Non-Linear Mech* 47:22–29
50. Mars WV (2002) Cracking energy density as a predictor of fatigue life under multiaxial conditions. *Rubber Chem Technol* 75:1–17
51. Wunde M, Klüppel M (2021) The role of phase morphology and energy dissipation around the crack tip in fatigue crack propagation of filler reinforced elastomer blends. In: Heinrich G, Stoček R, Kipscholl R (eds) *Fatigue crack growth in rubber materials: experiments and modelling*. Springer, Berlin
52. Windslow RJ, Hohenberger TW, Busfield JJC (2021) Determination of the loading mode dependence of the proportionality parameter for the tearing energy of embedded flaws in elastomers under multiaxial deformations. In: Heinrich G, Stoček R, Kipscholl R (eds) *Fatigue crack growth in rubber materials: experiments and modelling*. Springer, Berlin
53. Huneau B, Masquelier I, Marco Y, Le Saux V, Noizet S, Schiel C, Charrier P (2016) Fatigue crack initiation in a carbon black-filled natural rubber. *Rubber Chem Technol* 89:126–141
54. Ludwig M, Alshuth T, El Yaagoubi M, Juhre D (2015) Lifetime prediction of elastomers based on statistical occurrence of material defects. In: Marvalová B, Petříková I (eds) *Constitutive models for rubber IX*. CRC Press, Taylor & Francis Group, London, pp 445–448
55. Robertson CG, Tunnicliffe LB, Maciag L, Bauman MA, Miller K, Herd CR, Mars WV (2020) Characterizing distributions of tensile strength and crack precursor size to evaluate filler dispersion effects and reliability of rubber. *Polymers* 12:203
56. Ducrot E, Chen Y, Bulters M, Sijbesma RP, Creton C (2014) Toughening elastomers with sacrificial bonds and watching them break. *Science* 344:186–189
57. Xiang C, Wang Z, Yang C, Yao X, Wang Y, Suo Z (2020) Stretchable and fatigue-resistant materials. *Mater Today* 34:7–16
58. Das A, Sallat A, Böhme F, Suckow M, Basu D, Wießner S, Stöckelhuber KW, Voit B, Heinrich G (2015) Ionic modification turns commercial rubber into a self-healing material. *ACS Appl Mater Interfaces* 7:20623–20630
59. Zhang W, Liu X, Wang J, Tang J, Hu J, Lu T, Suo Z (2018) Fatigue of double-network hydrogels. *Eng Fract Mech* 187:74–93